Quantum Electronics **36** (3) 280 – 286 (2006) ©2006 Kvantovaya Elektronika and Turpion Ltd

PHOTODETECTION

PACS numbers: 42.50.Ar; 42.60.Da; 42.65.Sf
DOI: 10.1070/QE2006v036n03ABEH013135

Photodetection of a weak light signal in various quantum states by using an optical amplifier

A.V. Kozlovskii

Abstract. **The photodetection of weak light signals preliminary amplified in optical light amplifiers is analysed quantum-mechanically. A linear amplifier and a four-wave-mixing amplifier are considered. The parameters of the signal-to-noise ratio are calculated and analysed for light sources with various quantum-statistical properties. The signal-to-noise ratio for the detector photocurrent is studied as a function of the quantum-statistical properties of the signal and idler waves involved in amplification by using the four-wave-mixing scheme. The four-wave-mixing scheme with the idler wave in the coherent or Fock (squeezed, sub-Poisson) state has a higher signal-to-noise ratio compared to the linear preamplification regime.**

Keywords: *photodetection, quantum states, optical amplifier.*

1. Introduction

One of the methods for enhancing the sensitivity of photodetectors in the photon counting regime is based on the preamplification of an optical signal incident on the detector. In this case, the amplification of weak currents introducing the additional noise and thereby the additional error in the results of measurements can be avoided, which is very important for detecting weak and ultraweak optical signals. Laser amplification of radiation can be also used in optical communication systems for compensating for losses during the propagation of radiation in a fibre.

A laser amplifier introduces the additional noise due to spontaneous radiation in the active medium, which reduces its output signal-to-noise ratio. In this paper, we analysed quantum-mechanically the possibility of using a linear amplifier for preamplification of a weak light signal measured by a photodetector.

Another method for amplification of weak signals considered in this paper is based on nonlinear four-wave mixing of radiation in a cubically nonlinear medium. The use of the idler wave with certain quantum-statistical properties reduces the degree of signal degradation to the level acceptable for the subsequent measurement.

A.V. Kozlovskii P.N. Lebedev Physics Institute, Russian Academy of Sciences, Leninsky prosp. 53, 119991 Moscow, Russia;
e-mail: kozlovsk@sci.lebedev.ru

Received 20 July 2005; revision received 19 December 2005
Kvantovaya Elektronika **36** (3) 280 – 286 (2006)
Translated by M.N. Sapozhnikov

2. Quantum theory of photon counting

Let us analyse the single-mode photon counting regime that is realised when a measurement time of the number of photons is small compared to the coherence time of radiation at the input of an amplifier (i.e., the quantity inverse to the width of the radiation spectrum): $T \ll \tau_{\rm coh}$. We also assume that the photodetector area S in the single-mode photon counting regime is smaller than the area of spatial coherence of radiation: $S \ll S_{\rm coh}$. These conditions correspond to the approximation of a plane quasi-monochromatic wave at the amplifier input.

Consider the scheme of photodetection with a linear laser preamplifier in the single-mode approximation. The photon counting procedure involves a series of consequent measurements of the photocurrent resulting in the determination of the distribution of photoelectrons, which is directly related to the probability distribution of the number of field photons. Note that the distribution of photoelectrons obtained in this scheme does not coincide in the general case with the distribution of field photons at the photodetector input.

The distribution $p(m, T)$ of photoelectrons for a polyatomic broadband photodetector for the measurement time T can be obtained within the framework of the temporal perturbation theory (see, for example, [1, 2]). If the average number of photons during the time T is constant, i.e., $\langle m\rangle = \varepsilon\langle a^+a\rangle T$, then [1, 2]

$$p(m, T) = \int P(\alpha)\,\frac{\left(\varepsilon T|\alpha|^2\right)^m}{m!}\exp\left(-\varepsilon T|\alpha|^2\right){\rm d}^2\alpha, \qquad (1)$$

where $\langle|\alpha|^2\rangle = \langle a^+a\rangle$ is the number of photons in the quantisation volume $V_{\rm qu} = SL$; $L = cT$; and c is the speed of light. The parameter ε characterises the sensitivity of the broadband photodetector and is independent in the general case of the properties of the photodetector material and the frequency of the field being measured [1]. The Glauber – Sudarshan quasi-probability density function $P(\alpha)$ is defined in the phase space $\{\alpha_{\rm R}, \alpha_{\rm I}\}$ (where $\alpha = \alpha_{\rm R} + {\rm i}\alpha_{\rm I}$) and is directly related to the density operator of the electromagnetic field (statistical operator). Note that $\langle|\alpha|^2\rangle$ is calculated by using the P function, and $\langle a^+a\rangle$ – with the help of the density operator. The quantum efficiency η of the photodetector satisfies the relation $0 \leqslant \eta \leqslant 1$ and is determined by the expression $\eta = \varepsilon T$ assuming that the measurement time is shorter than the coherence time of the field.

It can be shown that the average number of photoelectrons is related to the average number of output photons of the laser amplifier by the expression $\langle m\rangle = \eta\langle n_a\rangle$, and photoelectron fluctuations are expressed in terms of photon fluctuations as

$$\langle \Delta m^2\rangle = \langle m\rangle(1-\eta) + \eta^2\langle\Delta n_a^2\rangle = \eta(\eta-1)\langle n_a\rangle + \eta^2\langle\Delta n_a^2\rangle. \quad (2)$$

In this case, the signal-to-noise ratio of the photodetector is described by the expression

$$\Re = \frac{\langle n_a^2\rangle}{(1-\eta)\eta^{-1}\langle n_a\rangle + \langle\Delta n_a^2\rangle}. \quad (3)$$

3. Amplified-radiation photon counting

3.1 Linear amplification in the single-mode regime

We will calculate $\Re$ by using the theory of laser amplification in the linear regime [2 – 5] to find the average quantities entering (3). For this purpose, we will employ the active-medium model of two-level atoms in the linear approximation with the transition frequencies close to the field frequency. By using the equation of motion for the annihilation operator of the quasi-monochromatic field in a laser amplifier [5], we find

$$\langle n_a\rangle = |G|^2\langle n_0\rangle + \mu, \quad (4)$$

where G is the gain; $\langle n_0\rangle$ is the average number of photons at the amplifier input;

$$\mu = \frac{N_\uparrow}{D}\left(|G|^2 - 1\right) \quad (5)$$

is the average number of spontaneous photons in the amplifier; $D = N_\uparrow - N_\downarrow$; $N_\uparrow$ and $N_\downarrow$ are the populations of the upper and lower levels of atoms in the active medium.

Fluctuations in the number of field photons at the amplifier output are expressed in terms of the average quantities at the amplifier input:

$$\langle\Delta n_a^2\rangle = \left[\langle\Delta n_0^2\rangle + u\left(1-|G|^{-2}\right) - \upsilon\right]|G|^4 + \upsilon, \quad (6)$$

where

$$u = \frac{N_\uparrow + N_\downarrow}{D}\left(\langle n_0\rangle + \frac{N_\uparrow}{D}\right); \quad (7)$$

$$\upsilon \equiv \frac{N_\uparrow N_\downarrow}{D^2}. \quad (8)$$

The gain of the laser amplifier is

$$G = \exp\left[\left(\frac{\kappa D}{2} - \mathrm{i}\omega\right)T_{\mathrm{amp}}\right], \quad (9)$$

where $D > 0$ is the population inversion maintained by pumping; $T_{\mathrm{amp}} = L_{\mathrm{amp}}/c_{\mathrm{m}}$ is the amplification time; L_{amp} is the amplifier length; c_{m} is the speed of light in the amplifier medium; ω is the transition frequency in the atom;

$$\kappa \equiv \frac{2g^2}{\Gamma}; \quad g = d\left(\frac{2\pi\omega}{\hbar V_{\mathrm{qu}}}\right)^{1/2}; \quad (10)$$

Γ is the spontaneous transition rate in the atom; and d is the dipole transition moment.

By substituting (4) – (8) into (3), we obtain the signal-to-noise ratio

$$\Re = \left(|G|^2\langle n_0\rangle + \mu\right)^2\left\{\frac{(1-\eta)}{\eta}\left(|G|^2\langle n_0\rangle + \mu\right) + \left\{\left[\langle\Delta n_0^2\rangle + ND^{-1}\left(1-|G|^{-2}\right)\langle n_0\rangle\right]|G|^4 + \mu(\mu+1)\right\}\right\}^{-1}, \quad (11)$$

where $N = N_\uparrow + N_\downarrow$. The quasi-probability distribution $P_{\mathrm{out}}(\alpha, t)$ of the field at the amplifier output is related to the quasi-probability distribution $P_{\mathrm{in}}(\alpha')$ of the field at the amplifier input by the expression

$$P_{\mathrm{out}}(\alpha, t) = \frac{1}{\pi\mu}\int \mathrm{d}^2\alpha' P_{\mathrm{in}}(\alpha')\exp\left(-\frac{|\alpha - G\alpha'|^2}{\mu}\right). \quad (12)$$

Below, we consider the following states of the input (measured) field: vacuum $|0\rangle$, the coherent state $|\alpha\rangle$, chaotic light $|\mathrm{Th}\rangle$, and a mixture of the coherent field with chaotic $|\alpha + \mathrm{Th}\rangle$ (signal + noise). To calculate the quasi-probability function, we find from (12) the average numbers of photons and their dispersions for the initial states $|0\rangle$, $|\alpha\rangle$, $|\mathrm{Th}\rangle$, and $|\alpha + \mathrm{Th}\rangle$ of the field being measured:

$$\langle n_0\rangle = \begin{cases} 0, \\ |\alpha_0|^2, \\ \langle n\rangle_{\mathrm{Th}}, \\ |\alpha_0|^2 + \langle n\rangle_{\mathrm{Th}}, \end{cases} \quad (13)$$

$$\langle\Delta n_0^2\rangle = \begin{cases} 0, \\ |\alpha_0|^2, \\ \langle n\rangle_{\mathrm{Th}}^2 + \langle n\rangle_{\mathrm{Th}}, \\ |\alpha_0|^2\left(2\langle n\rangle_{\mathrm{Th}} + 1\right) + \langle n\rangle_{\mathrm{Th}}(\langle n\rangle_{\mathrm{Th}} + 1). \end{cases} \quad (14)$$

The average numbers of photons and their dispersions at the amplifier output can be now calculated from expression (12) and

$$\langle\Delta n_a^2\rangle = |G|^4\langle\Delta n_0^2\rangle + |G|^2\left(1 - |G|^2 + 2\mu\right)\langle n_0\rangle. \quad (15)$$

In the case of a perfect amplification without introducing any noise into the amplified signal, the quasi-probability distribution $p_{\mathrm{id}}(n)$ (where n is the number of photons) is the initial distribution $p_0(n_0)$ with the substitution $\langle n_0\rangle \to |G|^2\langle n_0\rangle$. Note that in the case of an ideal photodetector ($\eta = 1$), the photoelectron distribution coincides with that of photons incident on the photodetector.

The calculations show that, when the number of incident photons is great (~ 100), the photoelectron distribution can be measured sufficiently accurately (Fig. 1), whereas in the case of weak signals with the number of photons ~ 1, photodetection with the use of a linear amplifier involves fundamental difficulties. One can see from Fig. 2 that the photoelectron distribution for a signal in the coherent state or the signal + noise state for $\langle n_0\rangle = 2$ drastically differs from that upon the ideal amplification of the same signal. In the case of very low signal-to-noise ratio, the photoelectron distribution in the amplified coherent signal almost coincides with the corresponding distribution for vacuum at the amplifier input. In this case, the probability of detecting the number of photons equal to zero (the absence of photocurrent) in one measurement does not virtually differ from the probability of detecting 1000 photons. It is obvious that it is impossible to establish the presence or absence of a signal under such conditions, taking into account the presence of the inevitable experimental error. The separation of a signal against the background is possible only in the case of a very high accuracy of photocurrent measurement and a great number of repeated measurements required to obtain an accurate statistical distribution. As follows from calculations, an increase in the inversion population of the active medium of a laser amplifier noticeably improves the measurement accuracy at large $\langle n_0 \rangle$.

If a signal is in the chaotic or thermal state, the situation is different. It follows from Fig. 3 that even upon a strong amplification of a weak signal with the chaotic quantum statistics, the photoelectron distribution weakly differs from that upon perfect amplification of this signal. However, as in the case of a coherent signal, to perform a reliable measurement, an extremely high accuracy of photon counting is required to distinguish the signal and vacuum photocurrents. As shown in Fig. 4, for $\langle n_0 \rangle \sim 100$, the photocurrent distribution and, hence, the result of photodetection for a chaotic signal differ only slightly from the corresponding dependence upon ideal amplification. In this case, photodetection is characterised by a low signal-to-noise ratio $\Re$.

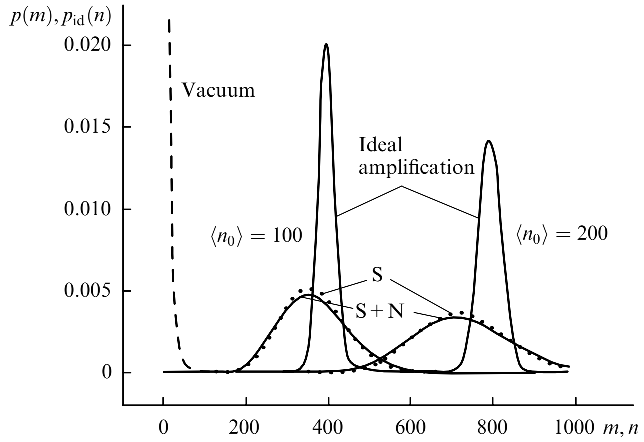

Figure 1. Distributions $p(m)$ of photoelectrons upon linear amplification of the input signal in the coherent state (S) and the signal + noise (S + N) state for the average number of photons at the amplifier input $\langle n_0 \rangle = 100$ and 200, $\langle n \rangle_{Th} = 0.388$, $|G|^2 = 4$, $\eta = 0.9$ and in the case of vacuum at the input. For comparison, the distributions of photons $p_{id}(n)$ in the case of ideal amplification are presented for the same parameters. The population inversion in the active medium of the laser amplifier is $D/N = 20\,\%$.

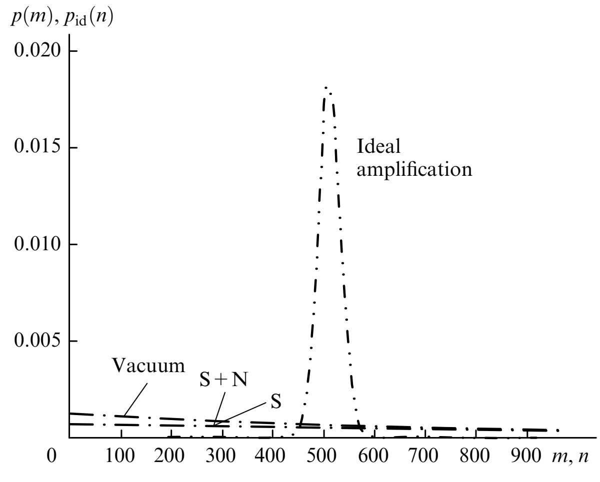

Figure 2. Same as in Fig. 1, for the input state of the signal + noise (S + N) field for $|G| = 16$, $\langle n \rangle_{Th} = 0.388$, $\langle n_0 \rangle = 2.388$, $\langle \Delta n_0^2 \rangle = 4.092$, $\Re = 1.16$, and the coherent input state of the field (S) for $\langle n_0 \rangle = 2$ and $\Re = 1.19$, and for the vacuum input field.

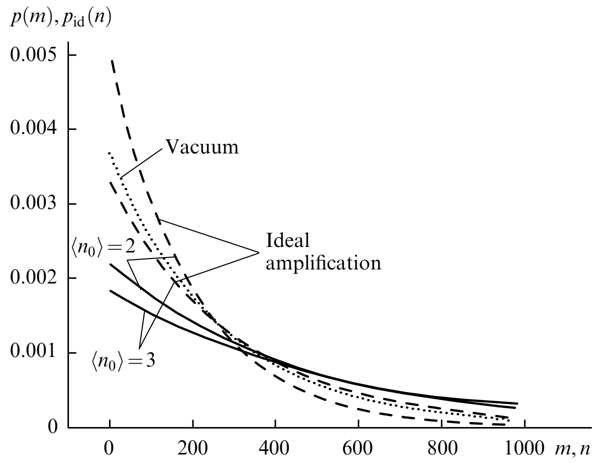

Figure 3. Same as in Fig. 1, for the input signal in the chaotic field state for $\langle n_0 \rangle = 2$ and 3, $|G|^2 = 100$, and for the vacuum input field.

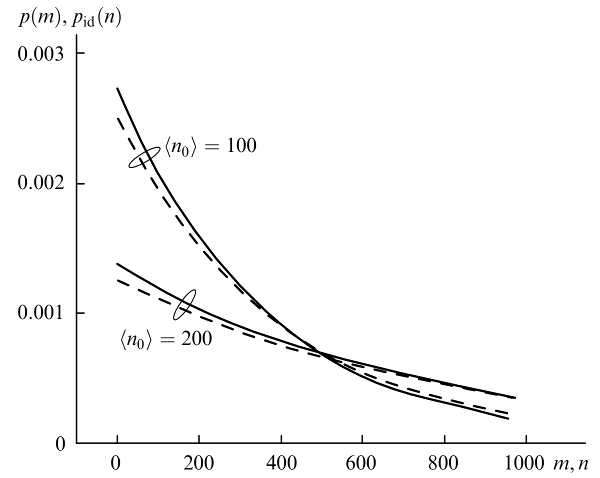

Figure 4. Comparison of the photoelectron distributions $p(m)$ for the chaotic state of the input signal (solid curves) with photon distributions $p_{id}(n)$ in the case of ideal amplification (dashed curves) for $\langle n_0 \rangle = 100$ and 200 and $|G|^2 = 4$.

One can see from Fig. 5 that for a chaotic signal $\Re$ drastically increases at very low gains and is equal to unity for large $|G|$. In the case of a coherent signal, the signal-to-noise ratio monotonically increases with increasing the average number of photons at a large gain.

3.2 Four-wave mixing

Consider now the scheme for weak-signal amplification by the four-wave-mixing method in a nonlinear medium of volume V_{amp} having the cubic nonlinearity $[\chi^{(3)}]$. The two

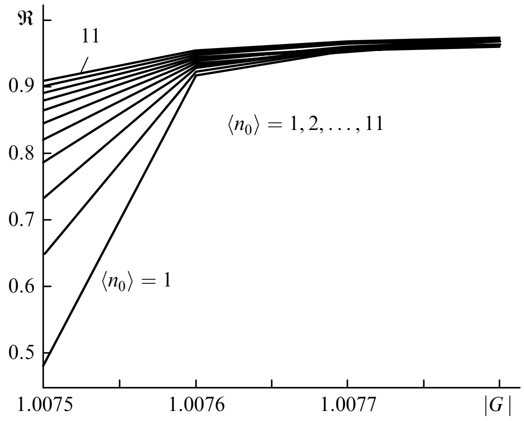

Figure 5. Dependences of the signal-to-noise ratio $\Re$ on the linear gain modulus $|G|$ for the chaotic signal for different $\langle n_0\rangle$ and $\eta = 0.9$.

intense counterpropagating pump waves with the amplitudes $E_{\rm p}$ and $E'_{\rm p}$ are mixed in a nonlinear medium with the counterpropagating signal and idler waves. It is assumed that the frequencies of the four quasi-monochromatic plane waves are identical, while the pump-wave intensities greatly exceed those of the signal and idler waves, so that we will consider the pump modes in the classical approximation by neglecting their depletion. Note that this approximation remains valid even in the case of strong amplification under the condition that the pump-wave intensities considerably exceed the intensities of the amplified waves. The operators a and d are the annihilation operators for the signal and idler modes of the electromagnetic field, while the operators c and b are the annihilation operators for the electromagnetic fields of the reflected and transmitted waves. The numbers of photons in the fields amplified upon degenerate four-wave mixing can be measured by direct photodetection.

The Heisenberg equations of motion for the annihilation operators $a(z)$ and $d(z)$ corresponding to the initial signal field $E_{\rm s}(z=0)$ and the initial idler field $E_{\rm i}(z=L)$ allow one to find the following relations for the input fields [2, 5]:

$$b \equiv a(z=L) = a\sec(KL) - \zeta d^{+}\tan(KL), \tag{16}$$

$$c \equiv d(z=L) = d\sec(KL) - \zeta a^{+}\tan(KL), \tag{17}$$

where

$$a \equiv a(z=0); \quad d \equiv d(z=L); \tag{18}$$

$$\zeta \equiv {\rm i}\exp[{\rm i}(\phi_{\rm p}+\phi'_{\rm p})]; \quad K \equiv \frac{\chi|E_{\rm p}E'_{\rm p}|}{c_{\rm m}}; \tag{19}$$

$\phi_{\rm p}$ and $\phi'_{\rm p}$ are the pump phases, and χ is the nonlinearity constant.

By using expressions (16) and (17), we find the average value and dispersion of the number of photons in the transmitted and reflected waves for different quantum states of the input fields. As the idler wave involved in four-wave mixing, we consider the fields in the purely coherent, Fock, and chaotic states. The state of the signal being measured is assumed coherent or chaotic.

In the general case, when the idler wave and signal field are in an arbitrary quantum state, we find the average value and dispersion of the number of photons in the amplified mode b in the form

$$\langle n_b\rangle = \langle b^{+}b\rangle = \sec^2(KL)\langle n_a\rangle + \tan^2(KL)(\langle n_d\rangle + 1)$$
$$- 2\sec(KL)\tan(KL){\rm Re}(\zeta^{*}\langle d\rangle\langle a\rangle), \tag{20}$$

$$\langle\Delta n_b^2\rangle = \langle n_b^2\rangle - \langle n_b\rangle^2 = \sec^4(KL)\langle\Delta n_a^2\rangle$$
$$+\tan^4(KL)\langle\Delta n_d^2\rangle - \big[4{\rm Re}(\zeta^{*}\langle d\rangle\langle a^{+}aa\rangle)$$
$$-2(2\langle n_a\rangle - 1){\rm Re}(\zeta^{*}\langle d\rangle\langle a\rangle)\big]\sec^3(KL)\tan(KL)$$
$$-\big[4{\rm Re}(\zeta^{*}\langle a\rangle\langle d^{+}dd\rangle) - 2(2\langle n_d\rangle - 1)$$
$$\times{\rm Re}(\zeta^{*}\langle d\rangle\langle a\rangle)\big]\sec(KL)\tan^3(KL)$$
$$+\big[\langle n_a\rangle\langle n_d\rangle + (\langle n_a\rangle+1)(\langle n_d\rangle+1)$$
$$+2{\rm Re}\big(\zeta^{*}\langle d^2\rangle\langle a^2\rangle\big) - 4{\rm Re}^2\big(\zeta^{*}\langle d\rangle\langle a\rangle\big)\big]. \tag{21}$$

The average value and dispersion ($\langle n_c\rangle$ and $\langle\Delta n_c^2\rangle$) of the number of photons for the second amplified wave can be obtained from the right-hand sides of (20) and (21) by the replacement $a \leftrightarrow d$.

If one of the fields (or both) is in the incoherent state (chaotic, vacuum, Fock, etc.), the equality $\langle x^{+n}x^{m}\rangle = 0$ takes place (where $x = a, d$; $n \neq m$ are positive integers) and expressions (20) and (21) are considerably simplified.

In the case of the coherent state $|\alpha,\delta\rangle$, the transformations

$$2{\rm Re}\big(\zeta^{*}\langle d^2\rangle\langle a^2\rangle\big) - 4{\rm Re}^2\big(\zeta^{*}\langle d\rangle\langle a\rangle\big)$$
$$= 2\langle n_a\rangle\langle n_d\rangle(\cos 2\Phi - 2\cos^2\Phi)],$$
$$2{\rm Re}(\zeta^{*}\langle d\rangle\langle a\rangle) = (\langle n_a\rangle\langle n_d\rangle)^{1/2}\cos\Phi \quad \text{etc.}$$

can be performed at the both inputs of a four-wave mixer in (21), where $\Phi = {\rm Arg}(\zeta^{*}\langle d\rangle\langle a\rangle)$.

If the idler mode is in the vacuum state $|0\rangle$, the expressions for the average number of photons and their fluctuations for the transmitted (b) and reflected (c) fields for an arbitrary state of the signal field coincide formally with the corresponding expressions (4) and (6) for a linear amplifier in which the substitutions $\mu \to \mu' \equiv \tan^2(KL)$ and $|G| \to |G'| \equiv \sec(KL)$ were performed. In this case, one can easily verify that, for the same gain $|G| = |G'|$, the average number μ of spontaneous photons for a linear amplifier coincides with the corresponding average number μ' for four-wave mixing upon the complete inversion of the active medium of the linear amplifier. As mentioned above, the signal-to-noise ratio upon photon counting and linear preamplification increases with increasing population inversion. This means that the use of a four-wave amplifier noticeably improves the accuracy of photocounts because the linear amplification regime is realised, as a rule, near the lasing threshold in the case of a weak population inversion in the medium.

Analysis of the signal-to-noise ratio $\mathfrak{R}$ (3) by using expressions (20) and (21) shows that $\mathfrak{R} = 1$ for the high gains ($|G'|^2 \gg 1$) and thermal states of both input fields. If the signal wave is in the thermal state and the idler wave is in the coherent state, then for $\langle n_d \rangle \gg \langle n_a \rangle$, $\langle n_d \rangle \gg 1$, and $\eta \approx 1$, we obtain

$$\mathfrak{R} = 1 + \frac{\langle n_d \rangle}{2(\langle n_a \rangle + 1)} \gg 1. \tag{22}$$

It follows from (22) that the use of the strong coherent idler wave in the case of small average numbers of photons in the signal field provides a high signal-to-noise ratio of the photocurrent. Figure 6 presents the dependences of $\mathfrak{R}$ on the gain modulus $|G'|$ and the average numbers of photons for the thermal signal and coherent idle waves. One can see that, unlike the case of linear amplification considered above, for high gains the maximum value of $\mathfrak{R}$ is achieved when the average number of photons in the signal field is minimal. This takes place both in the case of small and large average numbers of photons in the idler mode. One can also see from Fig. 6 that for $\langle n_a \rangle < \langle n_d \rangle$ (the number of photons in the signal wave is smaller than that in the coherent idler wave) and $|G'|^2 \gg 1$, the ratio $\mathfrak{R}$ decreases with increasing the number of signal photons, whereas for $\langle n_a \rangle \gg \langle n_d \rangle$, the ratio $\mathfrak{R}$ increases with $\langle n_d \rangle$. When the gain is weak, the ratio $\mathfrak{R}$ drastically decreases compare to its initial value ($|G'| = 1$) and then increases for $|G'| > 1$.

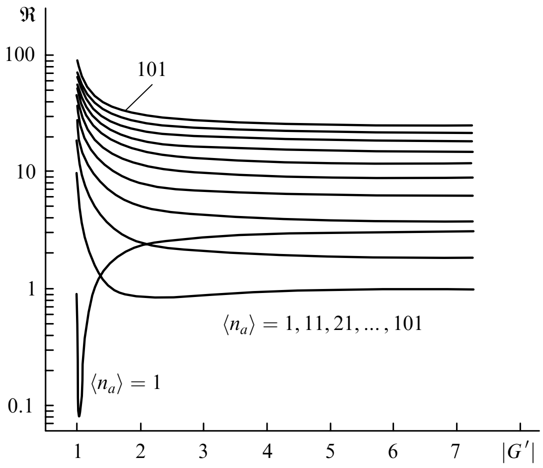

Figure 6. Dependences of the signal-to-noise ratio $\mathfrak{R}$ on the gain modulus $|G'|$ upon four-wave mixing of the thermal signal and coherent idler waves for different $\langle n_a \rangle$, $\langle n_d \rangle = 10$, and $\eta = 0.9$.

If the signal wave is in the coherent state and the idler wave is in the thermal state, a high signal-to-noise ratio cannot be achieved at small numbers of photons. In this case, we obtain

$$\mathfrak{R} = 1 + \frac{\langle n_a \rangle^2}{\langle n_d \rangle^2} \approx 1 \tag{23}$$

for $\langle n_d \rangle \gg \langle n_a \rangle$, $\langle n_d \rangle \gg 1$, and $\eta \approx 1$, and

$$\mathfrak{R} = 1 + \frac{\langle n_a \rangle}{2(\langle n_d \rangle + 1)} \gg 1 \tag{24}$$

for $\langle n_a \rangle \gg \langle n_d \rangle$ and $\langle n_a \rangle \gg 1$. This means that a high signal-to-noise ratio can be achieved only for a strong signal wave in the coherent state. Note also that, if $\langle n_d \rangle \approx \langle n_a \rangle$, then again $\mathfrak{R} \approx 1$.

Consider now the situation when the idler wave is in the Fock state with a certain number of photons. Then, we obtain from (20) and (21) that for $\langle n_a \rangle \gg \langle n_d \rangle$ and $|G'|^2 \gg 1$, the condition

$$\mathfrak{R} = \frac{\langle n_a \rangle}{2\langle n_d \rangle + 1} \gg 1$$

is fulfilled, whereas for $\langle n_d \rangle \gg \langle n_a \rangle$, we have $\mathfrak{R} \approx 1$. If the signal is in the thermal (chaotic) state, then $\mathfrak{R} \approx 1$ in the first case, and

$$\mathfrak{R} = \frac{\langle n_d \rangle}{2\langle n_a \rangle + 1}$$

in the second case.

Figure 7 shows the dependences of $\mathfrak{R}$ on $|G'|$ for different $\langle n_a \rangle$. A comparison of Figs 7 and 6 shows that for $\langle n_a \rangle = 1$ the ratio $\mathfrak{R}$ is higher for the idler wave in the Fock state and the coherent signal for $|G'|^2 \gg 1$. At the same time, for $\langle n_a \rangle > \langle n_d \rangle$, the signal-to-noise ratio is considerably higher when the coherent idler wave and thermal signal are used.

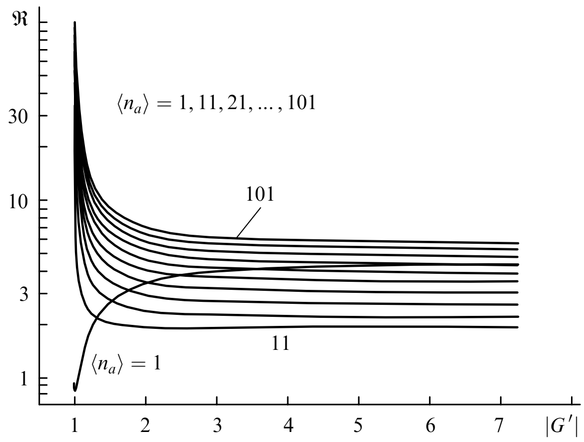

Figure 7. Same as in Fig. 6, for the coherent signal and idler wave in the Fock state.

Figure 8 shows the dependences of $\mathfrak{R}$ on $\langle n_a \rangle$ for different $\langle n_d \rangle$ and $|G'|^2 \gg 1$ when the signal is in the chaotic state and the idler wave is in the coherent state. One can see that the value of $\mathfrak{R}$ is very large when the idler wave with $\langle n_d \rangle \gg 1$ is used, but $\mathfrak{R}$ drastically decreases with increasing $\langle n_a \rangle$. Figure 9 presents the dependences of $\mathfrak{R}$ on $\langle n_a \rangle$ for different $\langle n_d \rangle$ for the Fock state of the idler wave and the coherent state of the signal. One can see that for small $\langle n_a \rangle$, the addition of the idler wave leads to the increase in $\mathfrak{R}$, while for large $\langle n_a \rangle$ – to the decrease in $\mathfrak{R}$.

If the signal and idler waves are in the coherent states $|\alpha\rangle$ and $|\delta\rangle$, respectively, the average number of photons is

$$\langle n_b \rangle = |G'|^2 \langle n_a \rangle + \left(|G'|^2 - 1\right)\langle n_d \rangle + \mu' - 2\cos\Phi\left[|G'|^2\left(|G'|^2 - 1\right)\langle n_a \rangle \langle n_d \rangle\right]^{1/2}, \tag{25}$$

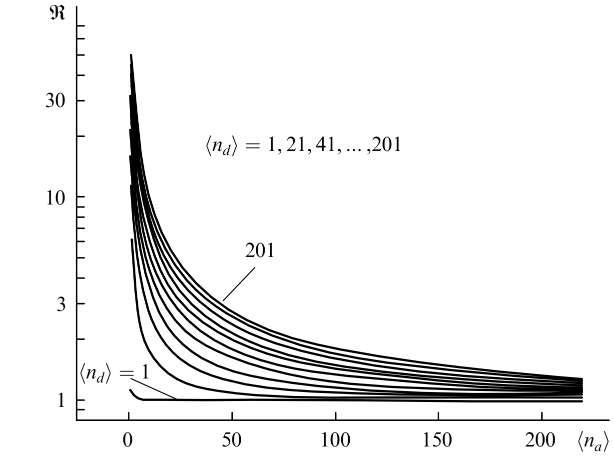

Figure 8. Dependences of the signal-to-noise ratio $\mathfrak{R}$ on the average number $\langle n_a \rangle$ of photons in the signal mode upon four-wave mixing of the thermal signal and coherent idler waves for different $\langle n_d \rangle$, $|G'|^2 \gg 1$, and $\eta = 0.9$.

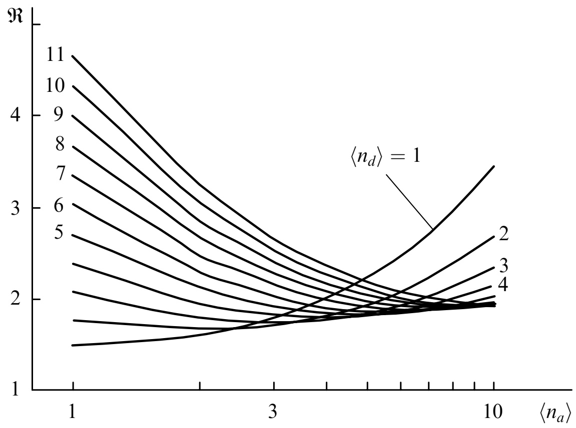

Figure 9. Same as in Fig. 8, for the coherent signal and Fock idler waves for different $\langle n_d \rangle$.

where

$$\Phi \equiv \phi_a + \phi_d - \phi_{\rm p} - \phi'_{\rm p} - \frac{\pi}{2};$$

ϕ_a and ϕ_d are the phases of signal and idler modes. The fluctuations of the number of photons in the propagating mode are described by the expression

$$\left\langle \Delta n_b^2 \right\rangle = |G'|^4 \left\langle \Delta n_a^2 \right\rangle + \left(|G'|^2 - 1\right)^2 \left\langle \Delta n_d^2 \right\rangle$$

$$+ \mu'(\mu' + 1)(\langle n_d \rangle + \langle n_a \rangle + 1)$$

$$- 2\left(2|G'|^2 - 1\right)\left[|G'|^2\left(|G'|^2 - 1\right)\langle n_a \rangle \langle n_d \rangle\right]^{1/2} \cos\Phi. \quad (26)$$

The expressions for $\langle n_c \rangle$ и $\left\langle \Delta n_c^2 \right\rangle$ can be obtained by the replacement $a \leftrightarrow d$ in (25) and (26).

It follows from (26) that the value of $\mathfrak{R}$ decreases with increasing $\langle n_a \rangle$ for $\langle n_d \rangle < \langle n_a \rangle$ and monotonically increases for $\langle n_d \rangle > \langle n_a \rangle$ if $\Phi = 2q\pi$ (where q is any integer). As a result, the signal-to-noise ratio takes large values for a small number of photons in the field being measured. At the same time, if the phase-matching condition of the type $\Phi = (2q+1)\pi$ is fulfilled, the dependence of $\mathfrak{R}$ on the average number $\langle n_a \rangle$ of photons has another character. As shown in Fig. 10, the ratio $\mathfrak{R}$ monotonically increases with $\langle n_a \rangle$.

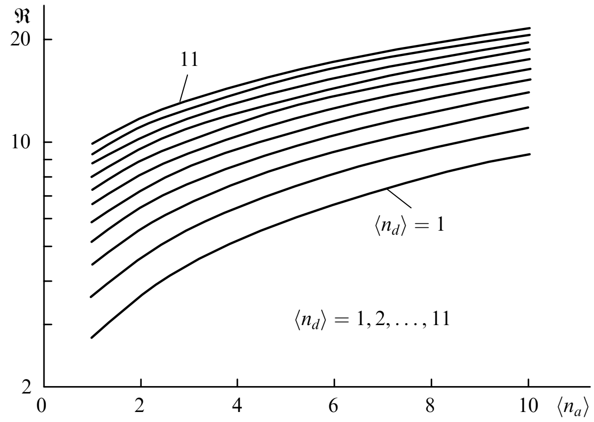

Figure 10. Same as in Fig. 8, for the coherent signal and idler waves upon phase matching of the type $\Phi = (2q+1)\pi$ and different $\langle n_d \rangle$.

It also follows from (26) that, if the intensities of the signal and idler waves are equal, the average number of photons in the propagating wave is equal to the square of the gain: $\langle n_b \rangle \approx |G'|^2$. In this case, the fluctuations of the number of photons are

$$\left\langle \Delta n_b^2 \right\rangle \approx 2|G'|^4 \langle n_b \rangle - |G'|^4. \quad (27)$$

It follows from (25) and (27) that these fluctuations always considerably exceed the shot noise level (super-Poisson statistics of the amplified field). At the same time, due to the effect described above [expressions (26) and (27)], the dependence of the signal-to-noise ratio on the average numbers of photons for $\Phi = 2q\pi$ acquires a complicated nonmonotonic character. The fluctuations in the number of photons approach thermal fluctuations when the average numbers of photons in the signal and idler waves are equal.

The measurement of the number of photons in the amplified wave gives complete information on their number in the input signal. Knowing the average number of photons in the idler wave at the second input of the amplifier, we find the average number of photons of the input field being measured directly from expression (20). The high signal-to-noise ratio of the photodetector is achieved by a proper choice of the quantum properties of the idler wave. A beamsplitter can be also used for this purpose. In this case, the initial signal is divided into two parts, each of them being directed to one of the inputs of a four-wave amplifier. The determination of the number of photons in the initial signal from the results of measurements of the amplified fields with the help of (20) under such conditions is simplified and does not require a preliminary measurement of the number of photons in the input idler wave.

4. Conclusions

Our analysis of the statistics of direct photodetection (photon counting) of the amplified signal has shown that a linear laser amplifier cannot be used for detecting weak signals containing a few photons and existing in the coherent or chaotic quantum state. In this case, when the signal gain is high, the result of a single measurement of the photocurrent proves to be indistinguishable within the experimental error from the result of measurement of the amplified vacuum or background thermal field. As the average number of photons in the measured volume is increased, photon counting becomes possible at the measurement accuracy achieved in practice for $\langle n_0 \rangle \sim 100$.

The study of the photodetection of a signal amplified in the four-wave-mixing scheme has shown that a weak signal (a few photons) can be measured with a high accuracy. In this case, the measurement accuracy, characterised by the signal-to-noise ratio of the detector photocurrent, depends qualitatively on the intensity and quantum-statistical properties of the idler wave. The mixing of the coherent or chaotic signal in the four-wave amplification scheme with the idler wave in the coherent or Fock state can lead to an increase in the signal-to-noise ratio of the photocurrent. The use of the Fock field as the idler wave allows one to increase the signal-to-noise ratio compared to the use of the idler wave in the coherent state, especially when the number of photons in the signal is small. If the field being measured is in the chaotic (thermal) quantum state, the coherent idler wave should be used in order to increase the signal-to-noise ratio.

In the case of coherent signal and idler waves, the phase matching of all the four coherent waves involved in the nonlinear process (including pump waves) is very important. In particular, if the sum of phases of the four interacting waves is $\Phi \approx (2q+1)\pi$ (where q is an integer) and the intensities of the signal and idler waves are equal, the signal-to-noise ratio of the amplified field proves to be extremely low (~ 1). At the same time, a high signal-to-noise ratio can be achieved when $\Phi \approx 2q\pi$ [5]. In the case of phase matching of the type $\Phi \approx (2q+1)\pi$ and equal intensities of the signal and idle waves, the output radiation intensity is independent of the intensity of a signal at the amplifier input and is determined only by the medium gain. Under such conditions, instead of amplification, the signal can be scattered with energy transfer from the signal and idler waves to pump waves.

Note that the noise characteristics of the field required for measuring weak signals can be obtained by means of a nonlinear laser amplifier. It is shown [6] that by selecting the optimal amplification length (or time), fluctuations introduced by spontaneous radiation during nonlinear amplification with saturation can be considerably reduced compared to the case of linear amplification. Note also that a four-wave amplifier has the advantage that upon strong amplification both output waves are identical. This allows the photodetection of one of the waves in optical communication systems without the distortion of another wave that carries information.

Various schemes for parametric amplification of weak optical signals without reducing the initial signal-to-noise ratio were considered in recent papers [7, 8].

Acknowledgements. This work was partially supported by the Program of the President of the Russian Federation for Support of the Leading Scientific Schools of Russia (Grant No. HSh-1512.2003.2).

References

1. Glauber R.J., in *Quantum Optics and Electronics* (New York: Gordon and Breach, 1965) p. 63.
2. Mandel L., Wolf E. *Optical Coherence and Quantum Optics* (Cambridge: Cambridge Univer. Press, 1995; Moscow: Fizmatlit, 2000).
3. Zel'dovich B.Ya., Sobel'man I.I. *Usp. Fiz. Nauk*, **101**, 1 (1970).
4. Caves C.M. *Phys. Rev. D*, **26**, 1817 (1982).
5. Kozlovskii A.V. *Zh. Eksp. Teor. Fiz.*, **129**, 30 (2006).
6. Kozlovskii A.V., Oraevsky A.N. *Zh. Eksp. Teor. Fiz.*, **109**, 1524 (1996).
7. McKinstrie C.J., Radic S., Raymer M.G. *Opt. Express*, **12**, 5037 (2004).
8. McKinstrie C.J., Yu M., Raymer M.G., Radic S. *Opt. Express*, **13**, 4986 (2005).